On the controversy of nanofluid rheological behavior

Leyla Raeisian[1], Jan Rudolf Eggers[1], Eckart Matthias Lange[1]*, Torsten Mattke[2], Andreas Bode[2], Stephan Kabelac[1]

[1] Institute of Thermodynamics, Leibniz University Hannover, Germany

[2] BASF SE, Ludwigshafen, Germany

* Corresponding author: lange@ift.uni-hannover.de

Abstract

Different findings about suitable correlations to describe nanofluid viscosity can be explained based on the research presented in this paper. The effective viscosity of nanofluids is crucial when nanofluids are considered as heat carrier fluids. Despite many publications however, no consensus about suitable correlations could be found in past years. Especially the impact of the shear rate on the viscosity is being discussed controversially. It is shown in this paper, that these different findings can be explained considering the theory for the rheology of suspensions. Any measurement of viscosity over shear rate only shows a section of the entire rheological behavior. Thus, experimental results of shear thinning, Newtonian behavior and shear thickening of nanofluids can all be a part of this overall range of possible shear rates. This hypothesis is validated based on viscosity data from literature and viscosity measurements over a wide range of shear rates for different nanofluids showing all three types of behavior.

Keywords: viscosity, shear rate, shear thinning, shear thickening, nanofluids

1. Introduction

Nanofluids, which are colloidal suspensions of metallic and/or nonmetallic nanoparticles with at least one dimension below 100 nm size dispersed in

conventional base fluids, are known for their considerable impact on transport mechanisms which usually improve heat transfer abilities. In detail the increase of the heat transfer surface area due to suspended nanoparticles, interaction and collision between nanoparticles and higher thermal conductivity of nanoparticles are the mechanisms that cause the heat transfer increase in nanofluids [1]. In this regard, researchers see some potentials for heat transfer applications due to an increase of thermal conductivity of the nanofluid compared with the base fluid. Other applications for nanoparticles are e.g. treatment of cancer by hypothermia or power generation using nanofluids as solar volumetric absorbers, as the optical properties of liquids can be strongly influenced by nanoparticles [2-4].

Most of the publications have focused on the thermal conductivity of nanofluids. However, it has been shown that viscosity as an important flow characteristic needs the same attention due to its vital impact on heat transfer. Therefore, viscosity of nanofluids should be thoroughly investigated and well understood before being used in practical heat transfer applications. Unfortunately, the experimental data published so far does not yield a consistent overall picture and there is no consensus about a unified correlation approach yet.

Viscosity is an important fluid property when analyzing the fluidic behavior. When a fluid is disturbed from an equilibrium state by a velocity u, the dynamic viscosity η describes the fluids tendency of energy dissipation [5]. In simple words, the dynamic viscosity is connected to the tangential force per area required to slide one layer A against another layer B with the fluid of interest in between.

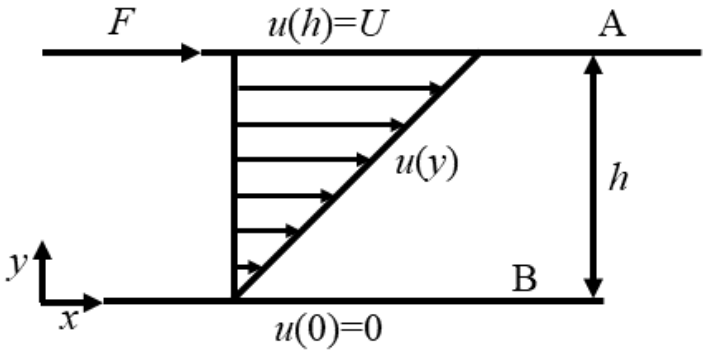

Figure 1 Simple shear of a liquid film between two plates

In Figure 1, the force F causing plate A moving with the velocity U in x-direction, creating a velocity profile in the liquid depending on y, is schematically shown.

So the viscosity of a fluid can be seen as the measure of how resistive the fluid is to flow, it can be defined by the mathematical expression

$$\eta = \frac{\tau}{\dot{\gamma}} \tag{1}$$

with the dynamic viscosity η in Pa·s, the shear stress τ in N/m and the shear rate $\dot{\gamma}$ in s^{-1}.

In one direction flow, the shear rate is generally expressed as:

$$\dot{\gamma} = \frac{\mathrm{d}u}{\mathrm{d}y} \tag{2}$$

where y is the height, t is the time, and $\mathrm{d}x/\mathrm{d}t$ is the velocity u. The flow characteristics of liquids are strongly dependent on the viscosity and are usually classified as follows:

a) Newtonian
b) Time independent Non-Newtonian
c) Time dependent Non-Newtonian.

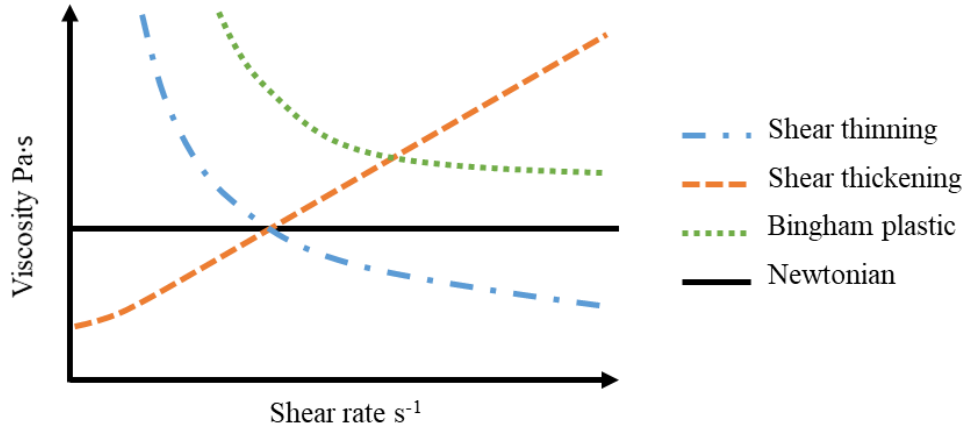

Figure 2 Different models for the change of viscosity with shear rate

According to Figure 2, when the viscosity of a liquid versus shear rate remains constant, the liquid is classified as Newtonian liquid. For non-Newtonian liquids, viscosity depends on the applied shear force and time. The most common types of time independent non-Newtonian liquids include: shear thinning fluids which display a decreasing viscosity with an increasing shear rate, shear thickening fluids in which viscosity increases with an increase in shear rate and Bingham plastic fluids where the fluid must be exposed to a certain amount of force to start to behave as a fluid. In time dependent non-Newtonian fluids viscosity changes with time as the fluid continues to undergo constant shear rate [6].

The Herschel-Bulkley model takes into account changes in the effective viscosity with the shear rate by assuming the power-law expressions [7]:

$$\eta = K\dot{\gamma}^{n-1} \tag{3}$$

where n is the power-law index and K is a consistency index. Depending on the value of the power-law index, the material flows as a shear-thinning fluid ($n<1$) or as a shear-thickening fluid ($n>1$). For $n=1$, the Herschel–Bulkley model reduces to a Newtonian behavior.

Unfortunately, theories of liquid viscosity are not well established so far, as a liquid is an intermediate state of matter between gas and solid, in which particles are attracted towards each other like solid particles but with less intermolecular forces of attraction. Due to the complex nature of this intermediate state of interaction on a molecular level, it is not easy to express the thermo-physical properties of liquids by physical sound theories. Theoretical methods of calculating liquid in line with the structure of a gas introduce a short-range pair distribution function in a disordered state of the fluid, as proposed by Kirkwood et al. [8,9] and Born and Green [10]. Moreover, Quiñones-Cisneros et al. [11,12] presented a new theory called “friction theory” by introducing the total viscosity as a combination of a dilute gas term as well as a friction term to calculate the fluid viscosity.

On the other hand, theories of liquid viscosity with solid-like structure supposed that each molecule is confined to small volumes as it interacts with a few neighbors only. So far, various researchers tried to explain fluids viscosity from this point of lattice- type of view like Brush [13], Eyrings et al. [14,15] and Collins [16]. Most of the pure theoretical models can hardly provide accurate results in ab initio approaches for viscosity of liquids. In contrast, semi-empirical and empirical methods present satisfactory results, but they lack a generality of approach. Semi-theoretical methods combine theoretical principles with experimental parameters and generally involve coupling of a viscosity model to other liquid characteristics. Most of these methods utilize corresponding state approach and/or the models are based on simplified statistical mechanics. Empirical equations involve variables like temperature, pressure, molecular mass and further properties like surface tension, vapor pressure and heat of vaporization [6]. In this regard, Guzman [17] proposed a very simple form for calculating the liquid viscosity as a function of temperature:

$$\eta = Ae^{(B/T)}. \tag{4}$$

Qun-Fang et al. [18] also suggested a two-parameters model to correlate the viscosity of pure saturated liquids over a wide temperature:

$$\ln\left(\frac{\eta V}{RT}\right) - \left(\frac{pV}{RT}\right) = \ln\left(\frac{1}{f}\right) + \left(\frac{\Delta U_{vap}}{RT}\right) \tag{5}$$

where V is the volume (m^3), R is the universal gas constant (J/mol·K), p is the pressure (Pa), f is the frequency (Hz) and ΔU_{vap} is internal energy of the liquid upon isothermal vaporization (J/mol).

Besides pure liquids, theories and correlations have been also suggested for the viscosity of suspensions, mixtures and solutions, which are often needed to design the different unit operations and processes involved [19-21]. The first

description of the effective viscosity η_{nf} of a fluid suspension with dispersed spheres dates back to Einstein [22, 23]:

$$\frac{\eta_{nf}}{\eta_{bf}} = 1 + 2.5\phi \tag{6}$$

in which η_{bf} is the base fluid viscosity and ϕ is the volumetric particle fraction. This approach is limited to non-interacting, spherical particles. The Einstein equation predicts viscosity with an uncertainty of less than ~6% for dilute solutions at volume particle fractions below 1 vol. %, in which no agglomeration occur [22,24]. In 1977 the equation was extended by Batchelor et al. to account for simple particle interactions (i.e. interactions between pairs of particles) in the fluid [25]. The extended equation is valid up to a volume fraction of 10 vol. % of particles [26]:

$$\frac{\eta_{nf}}{\eta_{bf}} = 1 + 2.5\phi + 6.2\phi^2 \tag{7}$$

The limited applicability of Eqs. (6) and (7) inspired many authors to develop enhanced formulations of the Einstein equation or develop completely new approaches, while all of the equations contain parameters which have to be fitted to experimental data. Reviews about these approaches are given by Khanafer et al. [27], Mahbubul et al. [28], Sundar et al. [29] and Mishra et al. [30]. Many of the given formulae are series expansions that simplify to Eq. 7 when higher order terms are neglected. However, these review articles conclude, that at present no theoretical model can predict the nanofluids viscosity sufficiently in a broad range of parameters.

According to the correlations and review papers mentioned above, some authors observed Newtonian viscosity behavior, whereas others noted shear thinning viscosity behavior, only a few of them measured shear thickening behavior in nanofluids. Prasher et al. [31] found, that Al_2O_3-propylene glycol nanofluids with up to 2 vol. % particle fraction show Newtonian behavior. This is in agreement with findings of Chandrasekar et al. [32] for Al_2O_3-water

nanofluids with up to 5 vol. %. Similar results are also shown by Anoop et al. [33] for Al_2O_3-water nanofluids with various particle fractions up to 6 vol. %. In contrast, Yang et al. [34] measured shear thinning behavior of Al_2O_3-water nanofluids with 1.28 vol. % at lower shear rates, but Newtonian behavior at higher shear rates. This viscosity behavior seems to be similar to that of Bingham-plastics, but it does not seem to be adequate to classify fluids of this type here, since the reproducibility of the effect is unknown yet. However, when Yang et al. reduced the effective particle size by adding stabilizer and thus limited agglomeration, the nanofluid showed Newtonian behavior over the complete range of shear rates between 10 and 1000 s^{-1}. Buschmann et al. [35] measured the viscosity of different nanofluid samples. Among them were higher concentrated samples (12.7 – 13.0 vol. %) of TiO_2- and Al_2O_3-nanofluids. They report that non-Newtonian behavior could be seen only at very low shear rates. In a benchmark test from 2009 several laboratories investigated SiO_2 nanoparticles in H_2O and Al_2O_3 nanoparticles in oil [36]. In the test, the SiO_2-H_2O nanofluid showed shear thinning behavior up to shear rate of about 10 s^{-1} and Newtonian behavior for higher shear rates whereas the Al_2O_3-oil nanofluid did not show significant deviation from Newtonian behavior in the range of between 0.1 to 1000 s^{-1}.

In contrast to the shear thinning and the Newtonian behavior of nanofluids, which were widely observed, shear thickening effects with increasing shear rates are not often mentioned in the literature. It was observed only by few researchers, for instance, it was described by Tseng et al. [37, 38] who reported a critical shear rate, at which viscosity begins to increase with shear rate. They found for Al_2O_3-water nanofluids, that the onset shear rate increases with the particle volume fraction. For volume fraction of 0.05 and a temperature of T = 25 °C they found the critical shear rate of about $\dot{\gamma}_m \approx 90$ s^{-1} at which shear thickening behavior begins. In another experiment, Tseng et al. [39] examined the viscosity of a dispersion of indium tin oxide (ITO) nanoparticles in water with 0.5–2 wt. % in

the presence of ammonium polyacrylate (NH_4PA) as a surfactant. From the result they concluded that critical shear-rate for the onset of dilatancy appears to reduce linearly with an increase of ϕ. A similar trend was presented for aqueous alumina and barium titanate suspensions with NH_4PA as surfactant [40]. In addition to Tseng et al. [41-43], who observed shear thickening behavior in nanofluids for the first time, some other researchers also reported shear thickening behavior of nanofluids [44-46] afterwards. Further findings from literature are summarized in Table 1.

Table 1 Reported behavior of CuO and Al_2O_3 nanofluid viscosity with the shear rate from literature.

Authors	**Nanoparticle/ base fluid**	**ϕ (vol. %)**	**Shear rate range(1/S)**	**Findings**	**surfactant**
Garg et al. [47]	CuO/EG	0.6, 1.5	3-3000	Nanofluid demonstrated a clear Newtonian behavior	No
Hojjat et al. [48]	Al_2O_3/H_2O CuO/H_2O	0.1, 0.5	350-950	An apparent shear thinning behavior was observed	No
Anoop et al. [33]	Al_2O_3/ H_2O Al_2O_3/EG CuO/EG	1, 4, 6	10-1000	Nanofluids showed an approximate Newtonian behavior	Not mentioned
Aladag et al. [44]	Al_2O_3/H_2O	1 wt %	0-4000	Nanofluid showed a strong shear thickening behavior over entire range	Yes
Namburu et al. [49]	$Al_2O_3/(H_2O$+ EG)	1, 2, 3, 4, 5, 6.12	0-8	Nanofluid indicated Newtonian behavior	No
Tseng and Wu. [38]	Al_2O_3/H_2O	3, 6, 11, 16	1-1000	Nanofluids showed shear thinning behavior in lower shear rate followed by shear thickening behavior in higher shear rates	No

Kole and Dey [50]	Al_2O_3/ engine oil	0.1, 0.4, 0.7, 1, 1.5	0- 90	For low Al_2O_3 loading, the nanofluid exhibited Newtonian behavior, while for higher loading (>0.004) shear thinning behavior was observed	Yes
Tseng and Wu [37]	Al_2O_3/H_2O	1, 3, 5, 10, 15	1-1000	Nanofluids exhibited a transition from shear thinning behavior to shear thickening behavior	No
Chandrasekar et al.[32]	Al_2O_3/H_2O	1, 2, 3, 4, 5	50-750	The nanofluid showed Newtonian behavior up to 2% volume fraction and for higher volume fraction a slight shear thickening was observed	No

To underline the problem of the proper interpretation of all data published, the viscosity of Al_2O_3/H_2O nanofluid as measured by Tseng and Wu [37] was compared with measurements by Hojjat et al. [48] in the range of 300 to 1000 s^{-1} in Figure 3 because of a comparable nanofluid and shear rate range. Despite these comparable boundary conditions, a contrasting behavior of the viscosity as a function of shear rate is observed. This might be due to different approaches of nanofluids preparation, e.g. stabilizers, nanoparticles properties or different methods of measurement.

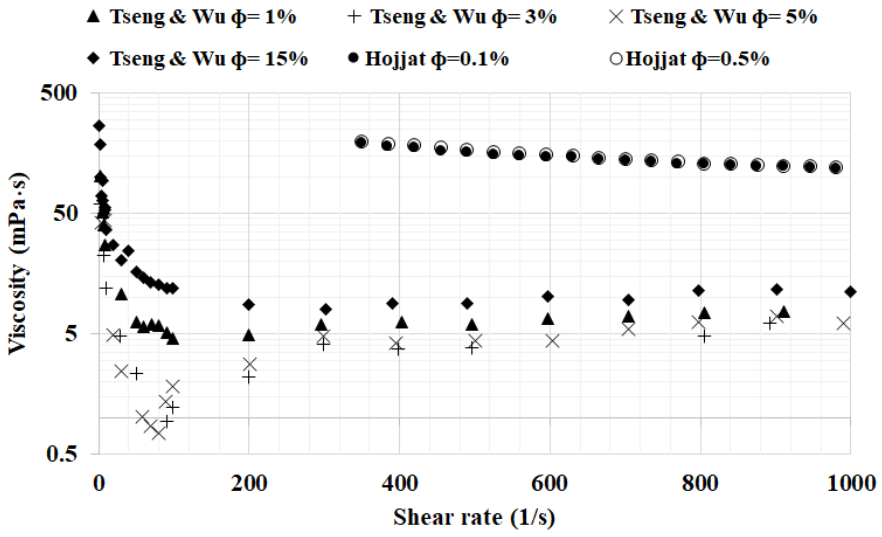

Figure 3 Comparison of Tseng and Wu [37] with Hojjat et al. [48] results

To investigate the rheological behavior, the viscosity of different types of nanofluids was measured in a wide range of volume fraction, temperature and shear rate. The results are then compared with literature data, followed by a discussion.

2. Experimental Procedure

The experimental results shown in this contribution have been gained with two different measurement procedures. Both sets of data were used later to give the heat transfer performance of these nanofluids. As the results were not satisfying regarding the heat transfer, the data on viscosity has never been published. However, more and more reports about Newtonian, shear thinning or shear thickening behavior emerged in the literature, so we now decided to re-analyze the existing data to shed some light on the matter of nanofluid viscosity.

The first set of data was recorded in the year 2002 at the Helmut-Schmidt University (HSU), the university of the Federal Armed Forces in Hamburg , Germany. Two different particle types were investigated. The first particle type were AEROSIL 200 SiO_2 nanoparticles and the second one were DEGUSSA c-type Al_2O_3 nanoparticles. Both particle types were dispersed in DI water as well as ethylene glycol. The Nanofluids were prepared by dispersing nanoparticles in proper concentrations in base fluids. After mixing them the suspension was homogenized by using a high performance mixer (model T25 digital ULTRA-TURRAX) for about 30 min to thoroughly mix the nanofluid. Then, nanofluids were stabilized by ultrasonic treatment and were kept in ultrasonic bath for about 2 h. Following this, a high power ultrasonication using an ultrasonic disruptor of KLN Sys 587 model was employed and inserted into the nanofluid solution for about 1 h. Further deagglomeration was carried out by passing the suspension through a high pressure shearing process in order to achieve a very homogeneous

nanofluid. Unfortunately, no measurement of the particles size distribution has been conducted at that time, the primary particle size is in both cases 20 nm.

The viscosity was measured using a USD200 (Physica) rheometer with the cone and plate geometry according to the standard of DIN 53019, where the cone diameter was 75 mm, the cone angle was 1° and the gap between cone and plate was 0.05 mm, as can be seen in Figure 4a. Measurements were conducted at different temperatures (20 °C – 60 °C), different shear rates (10 s^{-1} – 500 s^{-1}) and volume fractions of (0.5%, 1% and 2%). Every experiment was conducted twice to obtain more accurate results.

The second set of data is a measurement series conducted by the BASF Chemical Company in Ludwigshafen, Germany, in the year 2005. The nanofluids analyzed are an ethylene-glycol based CuO and a water based Al_2O_3 nanofluid which both were purchased from the U.S. company Nanophase Technologies Corporation. The CuO nanofluids were tested in volume fractions of 2.5%, 5% and 15%, the Al_2O_3 nanofluids were examined in volume fractions of 2.5%, 5%, 15.8%, 18.7% and 22%. The rheological analysis was performed over a temperature range of 25 °C – 80 °C using a Physica MC1 rheometer. The analyzed shear rates ranged from 0 to 1200 s^{-1}. Moreover, in order to observe possible hysteresis effects in the viscosity behavior, measurements with increasing and decreasing values of shear rates were performed.

The Physica MC1 double gap rheometer works according to DIN54433 and consists of concentric cylinders, it represents an accurate method of measuring the viscosity of nanofluids over a wide range of shear rates. According to the DIN standard, an inner cylinder is mounted in the center of a cup, thus, the cross section of the cup is showing an annular gap as it can be seen in Figure 4b. The rotating bob is like a hollow cylinder, therefore wetting both inner and outer surfaces which leads to an increase in shear area.

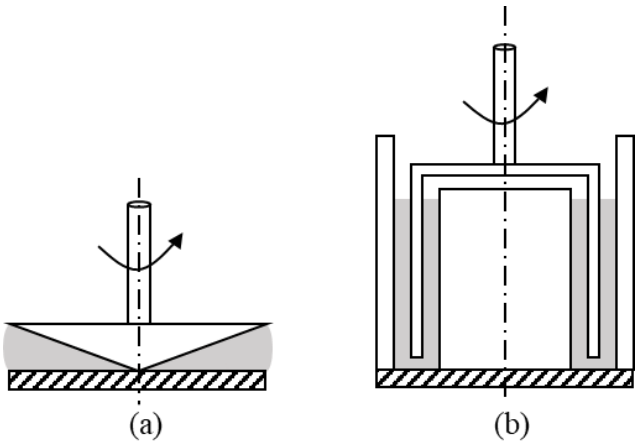

Figure 4 Schematic setup of measurement principle (a) according to DIN 53019 on the left side (b) according to DIN 54453 on the right side

The particle size distribution of the second set of nanofluids was measured using analytical ultracentrifugation. The results of these measurements are summarized in Table 2. The value D_{50} denotes the mean particle size, whereas the D_{10} and D_{90} provide information about the width of the size distribution.

Table 2 Particle size distribution from analytical ultracentrifugation

		Mass distribution	**Quantity distribution**
CuO in EG	D_{10} in nm	78	66
	D_{50} in nm	119	90
	D_{90} in nm	187	132
Al_2O_3 in H_2O	D_{10} in nm	55	49
	D_{50} in nm	91	61
	D_{90} in nm	170	96

3. Results and Discussion

In this part the results of the viscosity measurement are shown for both sets. Firstly, the viscosity results of SiO_2 in ethylene glycol, SiO_2 in water as well as Al_2O_3 in ethylene glycol and Al_2O_3 in water from Hamburg University of the Federal Armed Forces Germany are presented. Then, results of nanofluids

consisting of Al_2O_3 in water, CuO in ethylene glycol, from BASF company measurements are shown.

3.1. Viscosity measurement of the Hamburg University of the Federal Armed Forces Germany

The viscosity of SiO_2 and Al_2O_3 nanofluids with different particle volume fractions at temperatures between 20 °C to 60 °C were measured two times by employing the rotational viscometer for shear rates from 10 to 500 s^{-1}. Figures 5 and 6 show the results of the measurements for SiO_2 particles dispersed in ethylene glycol and water at the volume fraction of $\phi = 0.5\%$, respectively. As it can be seen, the viscosity of SiO_2-ethylene glycol shows only a minimal influence of shear thinning, whereas for SiO_2-water nanofluid a clear shear thinning behavior is observed.

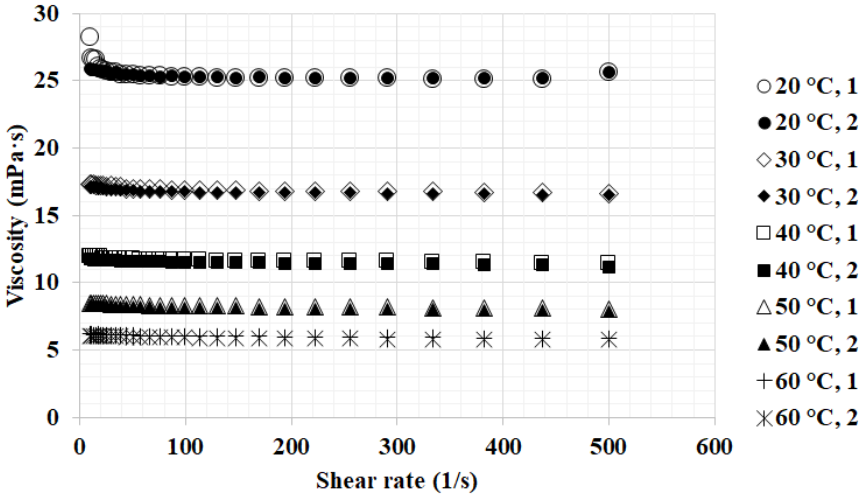

Figure 5 Measured viscosity of a SiO_2- ethylene glycol nanofluid with $\phi = 0.5\%$, all measurements were performed two times labeled with 1 and 2

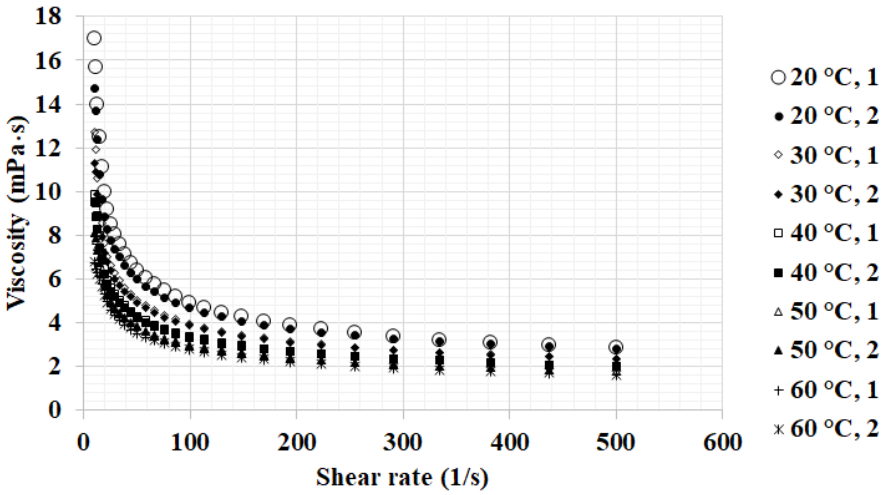

Figure 6 Measured viscosity of a SiO_2- water nanofluid with ϕ = 0.5%, all measurements were performed two times labeled with 1 and 2

Measurement results for Al_2O_3- water and Al_2O_3- ethylene glycol nanofluids at the volume fraction of ϕ = 0.5% are shown in Figures 7 and 8. For Al_2O_3- water nanofluid in Figure 7, shear thinning behavior is observed at low shear rates, changing to Newtonian behavior at moderate shear rates and to obvious shear thickening behavior at higher shear rates. Whereas, for Al_2O_3- ethylene glycol nanofluid shear thinning behavior followed by Newtonian behavior can be seen for temperatures of 30 °C to 60 °C. Only for a temperature of 20 °C all three types of rheological behavior are observed to a minor extend (Figure 8).

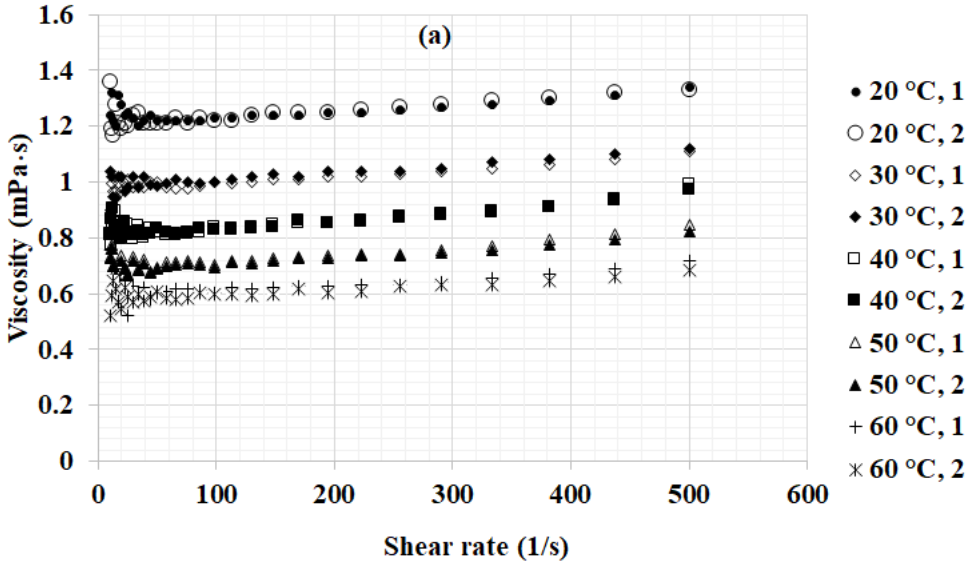

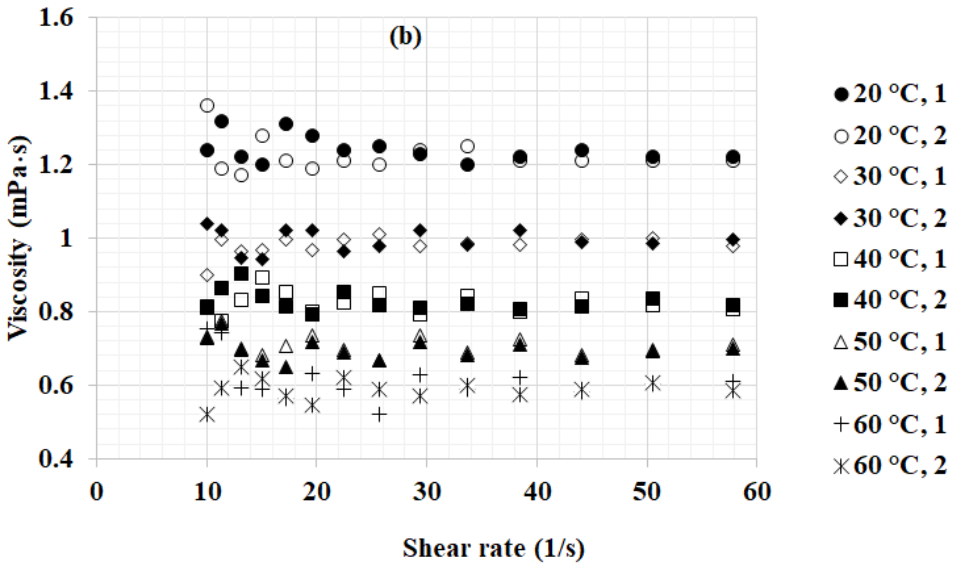

Figure 7 Measured viscosity of a Al_2O_3- water nanofluid with $\phi = 0.5\%$, all measurements were performed two times labeled with 1 and 2. (a) in a shear rate range from 5 s^{-1} to 500 s^{-1} (b) in the range of 5 s^{-1} to 60 s^{-1} of shear rate

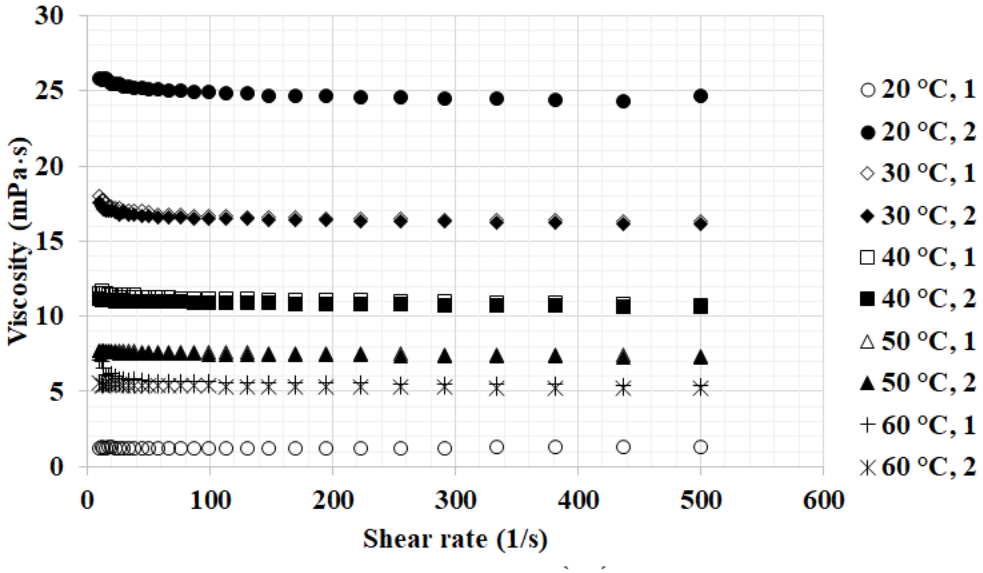

Figure 8 Measured viscosity of a Al_2O_3- ethylene glycol nanofluid with $\phi = 0.5\%$, all measurements were performed two times labeled with 1 and 2

Moreover, experimental results for Al_2O_3- ethylene glycol at a volume fraction of $\phi = 1\%$ and Al_2O_3- water at the volume fraction of $\phi = 2\%$ are shown in Figures 9 and 10, respectively. In both nanofluids shear thinning behavior is observed, however it is more obvious in the Al_2O_3- water nanofluid.

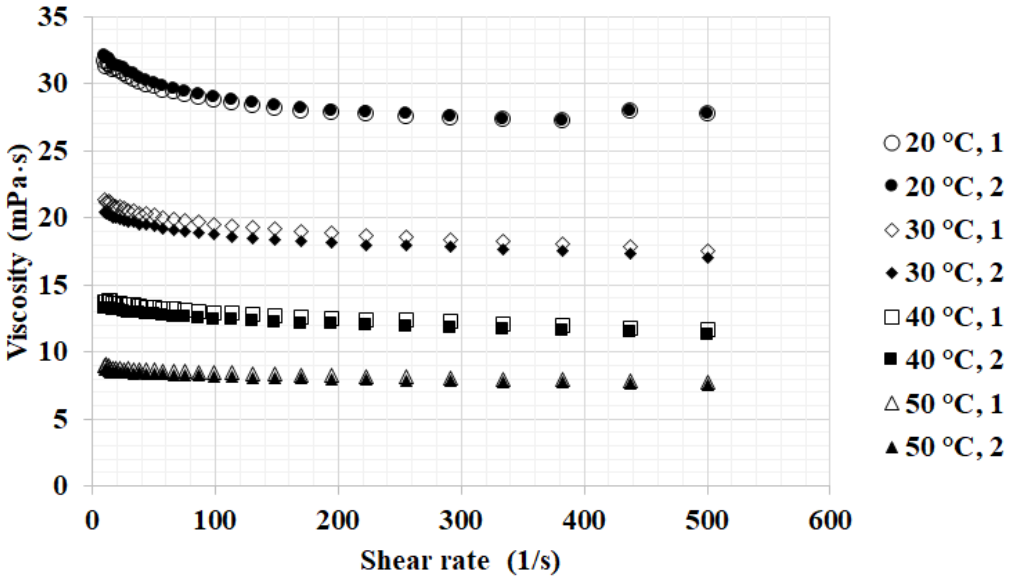

Figure 9 Measured viscosity of a Al_2O_3- ethylene glycol nanofluid with ϕ = 1%, all measurements were performed two times labeled with 1 and 2

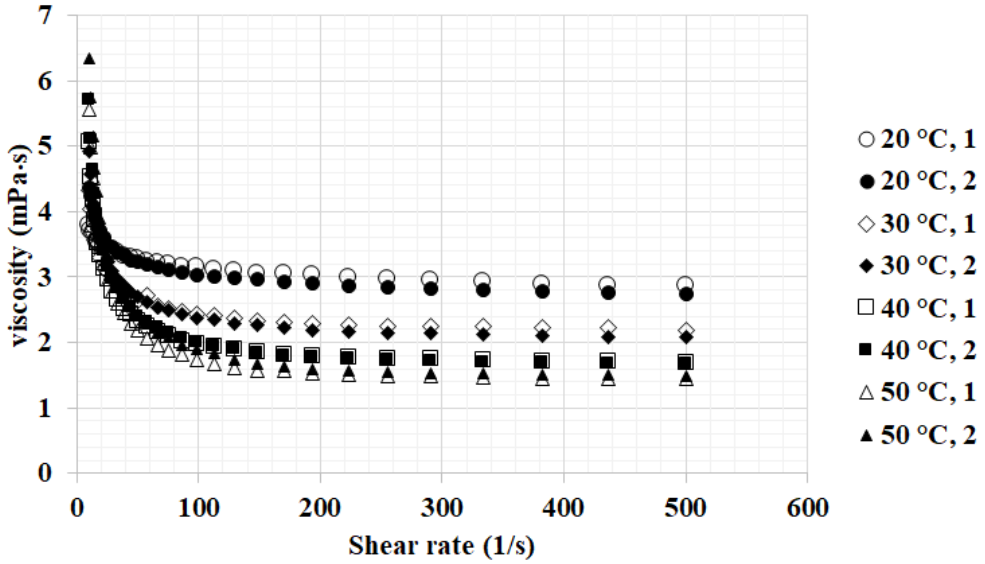

Figure 10 Measured viscosity of a Al_2O_3- water nanofluid with ϕ = 2%, all measurements were performed two times labeled with 1 and 2

3.2.Viscosity measurement of the BASF Company

In this section the results of the viscosity measurements at the BASF Company are shown. The results of BASF are split into two sections, beginning with lower volume fractions ϕ<10%, followed by higher volume fractions ϕ>10%.

3.2.1. Viscosity measurement for volume fractions < 10%

Using a double gap viscometer, the viscosities of Al_2O_3 and CuO nanofluids with different particle concentrations at temperature of 25 °C, 50 °C and 80 °C were measured for increasing (up) and decreasing (down) shear rates. Figure 11 shows the results of the measurements for CuO particles dispersed in ethylene glycol at the volume fraction of ϕ = 2.5% for three different temperatures of 25 °C, 50 °C, and 80 °C. At low shear rates, shear thinning behavior can be seen, changing to Newtonian behavior at higher shear rates. Moreover, small hysteresis effects can be seen, which will be discussed later. Also, a slight increase in viscosity is observable towards higher shear rates at T = 80 °C. Recalling the model fluids shown in Figure 2, the description of a Bingham plastic would suit the shown data best. However, this expression will not be used in the following, since the effects causing the shear thinning maybe not fluid-intrinsic, but are possibly produced by complex particle interactions that are not entirely known yet.

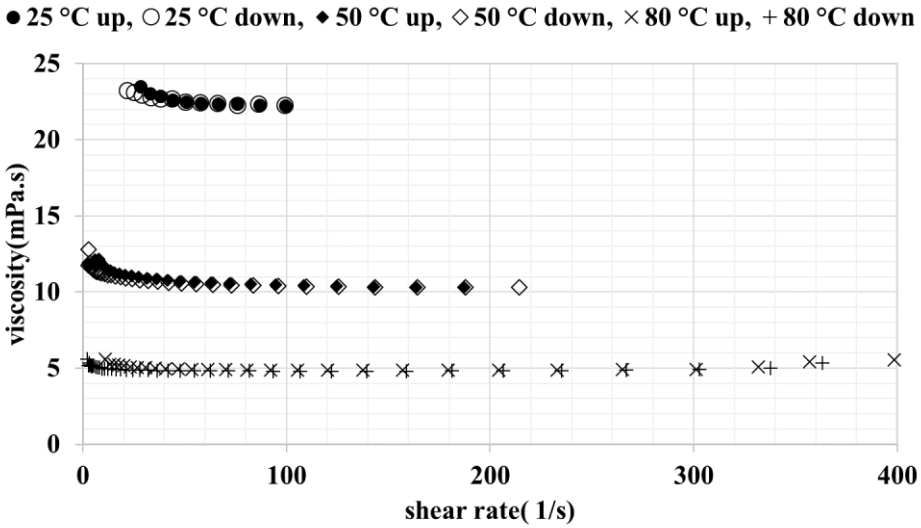

Figure 11 Measured viscosity of a CuO- ethylene glycol nanofluid with ϕ = 2.5%

Measurements for CuO in ethylene glycol were repeated with a higher volume fraction of ϕ = 5% for a wider range of shear rates according to Figure 12.

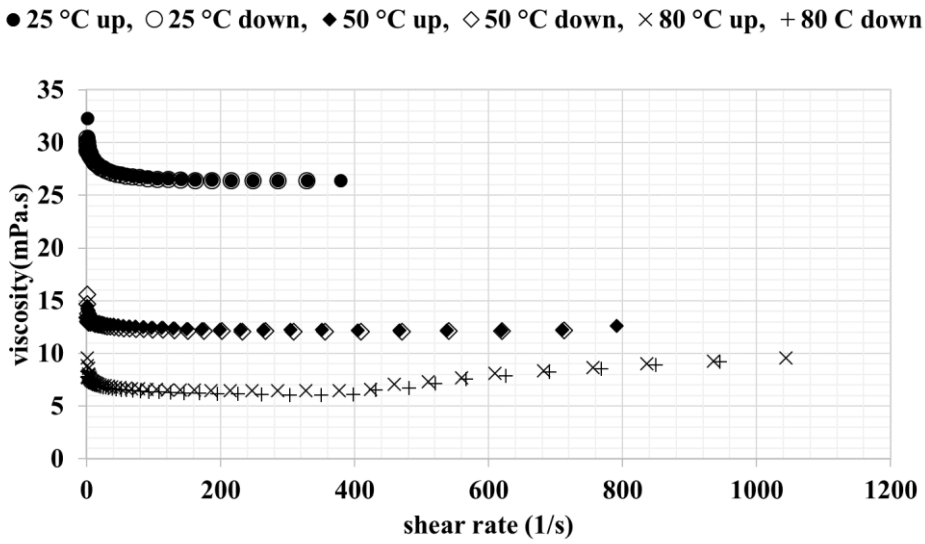

Figure 12 Measured viscosity of a CuO- ethylene glycol nanofluid with ϕ = 5%

Similar to the results obtained for ϕ = 2.5%, shear thinning behavior is observed at low shear rates, followed by Newtonian behavior at moderate shear rates and slight shear thickening behavior at higher shear rates. It is also worth noting that an increase of temperature leads to an onset of shear thickening behavior at lower shear rates. The results for a particle fraction of ϕ = 5% of Al_2O_3 particles in water are presented in Figure 13. The measurement results of Al_2O_3 particles in water are a good example to observe three distinct rheological behaviors of nanofluids clearly. Furthermore, strong hysteresis effects can also be identified from these results. The discussion of these observations follows in chapter 3.3.

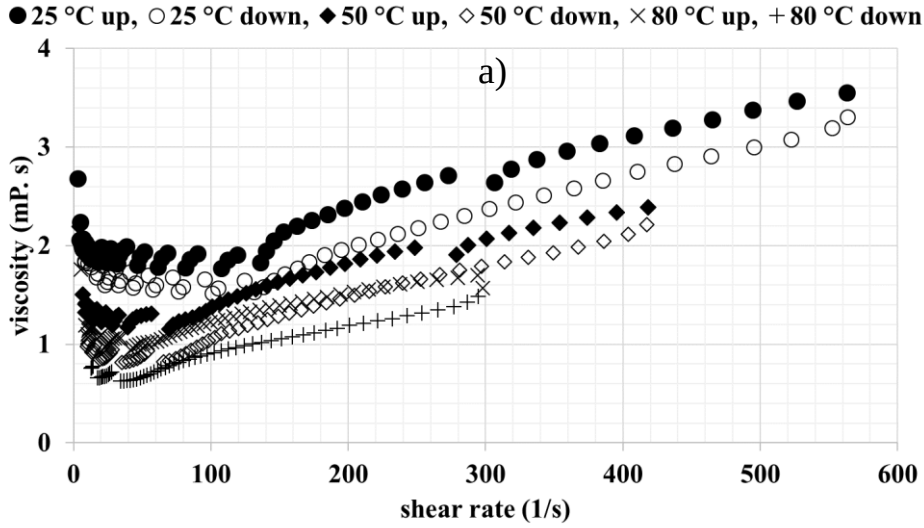

336

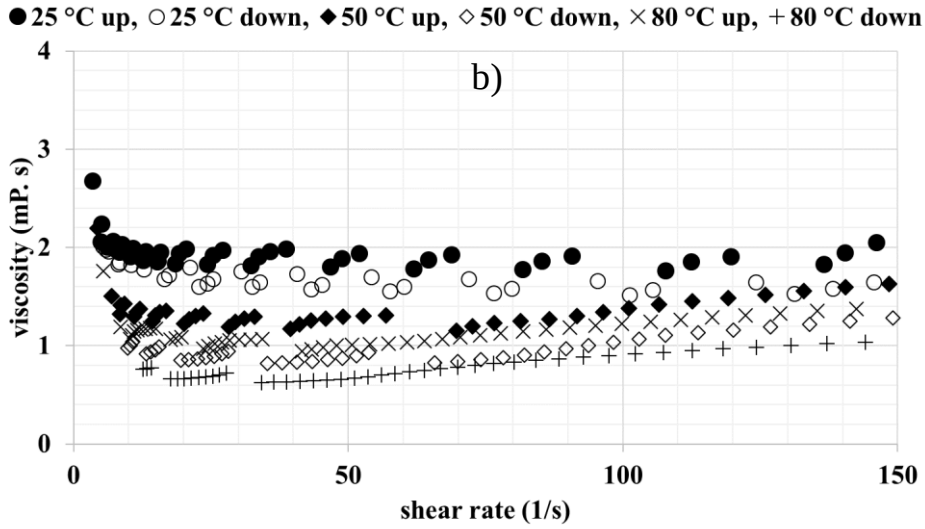

337

338 **Figure 13** Measured viscosity of Al_2O_3-water nanofluid with ϕ = 5% in a shear range of a) 0
339 to 600 s^{-1} and in the range of b) 0 to 150 s^{-1}

340 ### 3.2.2. Viscosity measurements for volume fraction > 10%

341 In the following, measurement results for volume fractions higher than 10% are
342 shown. Measured viscosity data for Al_2O_3 –water nanofluids with ϕ = 15.8%,
343 ϕ = 18.7% and ϕ =22% at 25 °C are shown in Figure 14.

344

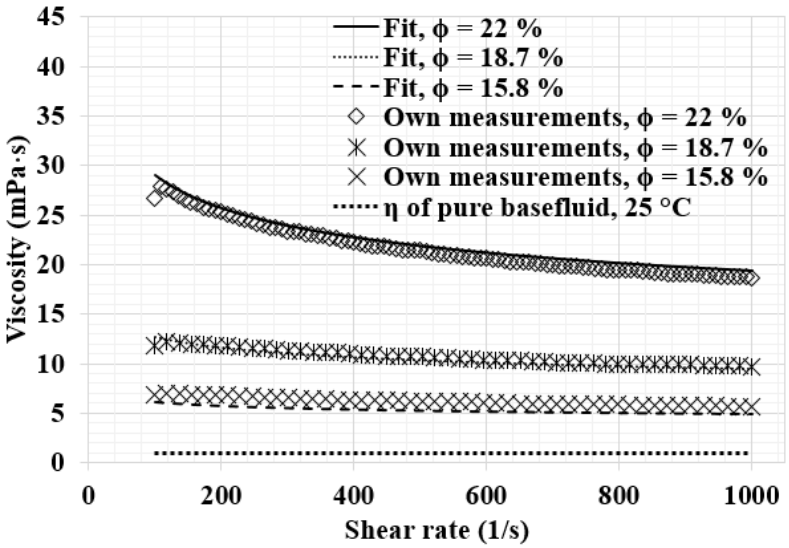

Figure 14 Measured viscosity of Al_2O_3 – water nanofluids for volume fractions > 10% at 25°C over shear rate vs. least square fit (Eq. 9)

Strong shear thinning behavior is observed for ϕ=22%, whereas for lower particle concentrations the fluids tend to Newtonian behavior. In such cases, a power law equation can be fitted to the measured data using a least square fit, in which the concentration of nanoparticles has to be inserted as a volume fraction:

$$\begin{aligned} \eta &= k \cdot \dot{\gamma}^{n-1} \\ k &= \eta_{\mathrm{bf}}(1 + A_{\mathrm{k}} - A_{\mathrm{k}} \exp(B_{\mathrm{k}}\varphi)) \\ n &= \sqrt{1 - A_{\mathrm{n}}\varphi} \\ A_{\mathrm{k}} &= -0.049002,\ B_{\mathrm{k}} = 33.30365,\ A_{\mathrm{n}} = 6.67627 \end{aligned} \tag{8}$$

Moreover, results of viscosity measurements for CuO nanoparticles in ethylene glycol at different shear rates are shown in Figure 15. The viscosity data axes are scaled logarithmically, while shear rates are shown in logarithmic scaling in Figure 15a, and in linear scaling in Figure 15b. The particle volume fraction of the nanofluid samples is ϕ = 15%. As for the Al_2O_3-water nanofluids, the data are correlated using a power law approach, the fitted equations for the CuO – ethylene glycol nanofluids are:

$$\eta = k \cdot \dot{\gamma}^{n-1}$$
$$k = A_k - B_k \eta_{\mathrm{bf}} + C_k \eta_{bf}^2$$
$$n = A_n + B_n \eta_{bf} + C_n \eta_{bf}^2 \qquad (9)$$
$$A_{\mathrm{k}}=12.5369,\ B_{\mathrm{k}} = 905.049,\ C_{\mathrm{k}} = 28806$$
$$A_n=0.143899,\ B_{\mathrm{n}} = 4.86454,\ C_{\mathrm{n}} = 223.295$$

In Figure 15, values for CuO – ethylene glycol are shown for 25 °C, 50 °C and 80 °C, respectively. The base fluid viscosity data is a function of the temperature and therefore accounts for the temperature dependence of the given curve fits. Similar to the values recorded for Al_2O_3, the CuO ethylene glycol nanofluid has a shear thinning behavior with a seemingly asymptotical trend towards high shear rates.

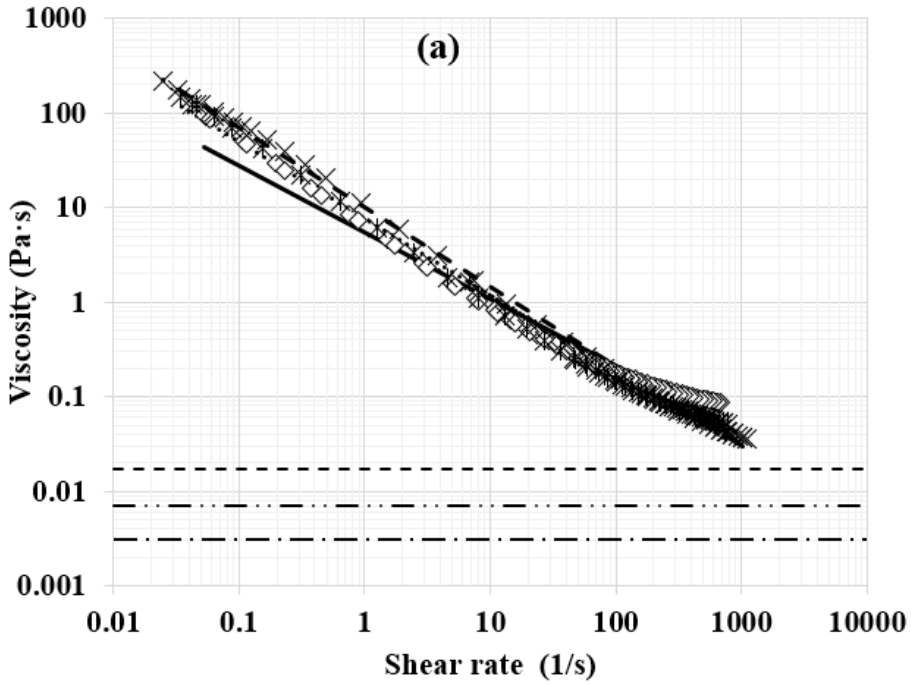

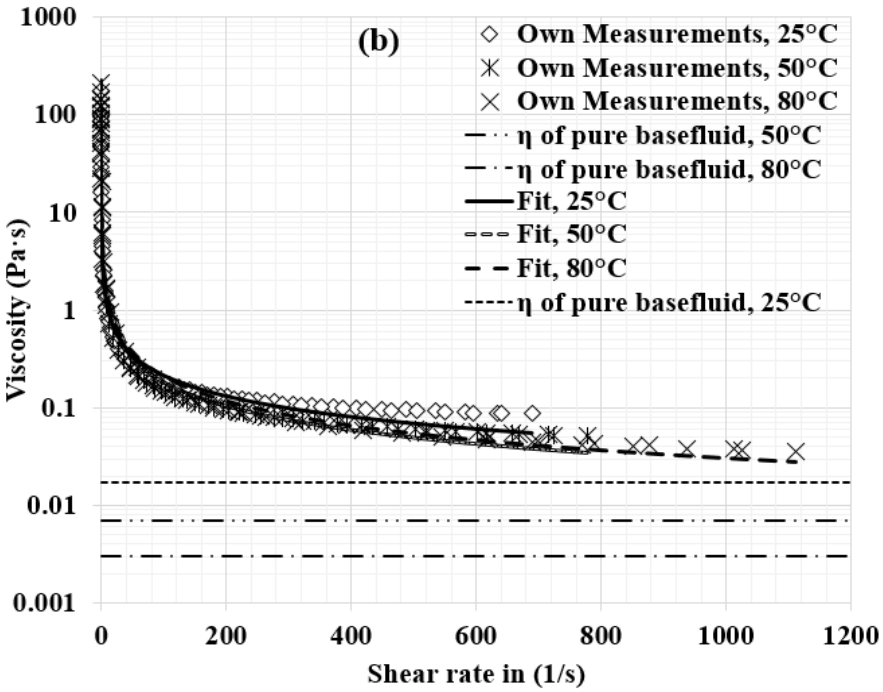

Figure 15 Measured viscosities of CuO-ethylene glycol nanofluids with $\phi = 15\%$ and the viscosities of pure ethylene glycol at different temperatures, as a function of the shear rate vs. least square fit (Eq. 10) (a) logarithmically (b) linearly scaled abscissa.

3.3. Analysis of experimental viscosity data

First, the hysteresis effect in the measurements of a nanofluid is addressed. This effect has been observed for example by Nguyen et al., when nanofluids are heated above a "critical" temperature. Somewhat lower viscosities of Al_2O_3-water and CuO-water nanofluids were measured in the heating phase than in the subsequent cooling phase [51,52]. Hysteresis effects can also be seen in the measurements presented in this paper for increasing and decreasing shear rates, especially at elevated temperatures and higher shear rates. At decreasing shear rates, the viscosity is measured to be lower than at increasing shear rates. As measurements were conducted isothermally, the effect mentioned by Nguyen et al. cannot explain our findings. A possible explanation for this effect is agglomeration. At high shear rates, agglomerates are destroyed leading to better dispersion and thus leading to a decreased viscosity (see especially Figure 13).

Another remarkable behavior is the combination of shear thinning and shear thickening behavior that can be observed in several measurements.

The measurements confirm the expected rheological behavior of a suspension that is described in the literature and comprehensively summarized by Barnes [7]. As it was mentioned before, nanofluids are classified as colloidal suspensions of nanoparticles in base fluids. He states that, with increasing shear rate, particles will begin to align in layers, which leads to a decrease of viscosity (shear thinning), which can last for several magnitudes of shear rates. This can actually be confirmed by most of the measurements shown above. At some point of shear rate, the transition is complete, no more alignment will occur and Newtonian behavior will be observed. The presence of such a Newtonian plateau can also be seen in the current measurements. At higher shear rates the layering is destroyed because of turbulence, and the particles will distribute randomly which results in an increase of viscosity. Such shear thickening behavior could be identified in many of our measurements. It can be concluded that if measurements are conducted at appropriate shear rates, nanofluids will show Newtonian, shear thinning or shear thickening behavior as well. Brown et al. [53] believed that all suspensions are supposed to exhibit shear thickening behavior under appropriate conditions. On the basis of experiments, they concluded that yield stress, which is the shear stress at the starting value of shear rate from zero, directly determines the advent of shear thickening region, as an increase of yield stress pushes the onset of shear thickening to higher values of shear rate. The yield stress also depends on various parameters such as volume fraction of particles, particles size, particle shape, surfactant and etc. which were mentioned by Brown et al.[53] as well as by Barnes [7]. Brown et al. [53] also suggested a correlation to show the interplay between yield stress, shear thinning and shear thickening behavior as follows:

$$\tau_{\mathrm{m}} = \tau_{\mathrm{HB}}\left(\dot{\gamma}_{m}\right) + \frac{\varepsilon}{2(1-\varepsilon)}\left(\tau_{\mathrm{HB}}\left(\dot{\gamma}_{m}\right) + \tau_{\mathrm{y}}\right) \tag{10}$$

where τ_{m} indicates the lower boundary of the shear thickening region that takes place at the shear rate of $\dot{\gamma}_{m}$ according to a minimum viscosity. ε is a model parameter, τ_{HB} and τ_{y} are shear thinning stress and yield stress, respectively. Wagner and Brady [54] also conducted a study to explain the shear thickening phenomena from a more practical point of view. They believe that all suspensions have a common behavior as a function of the shear rate as shown qualitively in Figure 16. In an equilibrium state the inter-particle forces including electrostatics and van-der-Waals forces are stronger than hydrodynamic interactions, so that the particles distribute randomly and the resistance to flow is rather high. By increasing the shear rate, the nanoparticles rearrange in parallel line in flow which lowers the viscosity and the suspension exhibit the shear thinning behavior. With more increase of shear rate the hydrodynamic interactions dominate over the inter-particle forces that drive Brownian motions and severe hydrodynamic coupling between particles result in creation of hydro-clusters which are the apparent features of shear thickening state.

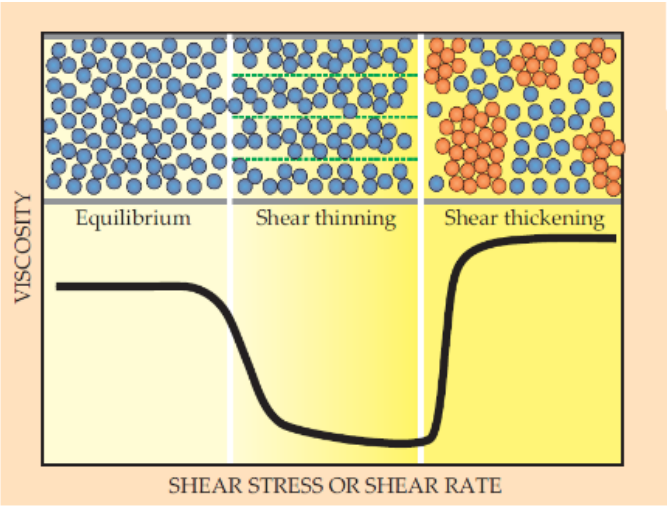

Figure 16 Microstructure of colloidal dispersion at different shear rates [54]

Their findings is in agreement with the work of Foss and Brady [55], which concentrates on the simulation of viscosity of suspensions, considering the influence of Brownian motion and hydrodynamic effects. The simulation results, that are based on prior investigations by Brady, Phung and others, are shown in Figure 17 [56]. Without elaborating on Stokesian dynamics or the hard sphere model, it can be seen that Brownian viscosity η_B decreases at low Peclet numbers (Pe), whereas the hydrodynamic viscosity η_H increases with the Peclet number. The two effects result in a local minimum of viscosity. The Peclet number is defined as

$$\mathrm{Pe} = 6\pi\eta a^3\dot{\gamma} / (k_B T) \tag{11}$$

with the Boltzmann constant k_B and the particle radius a and can be seen as the ratio of Brownian and flow time scales.

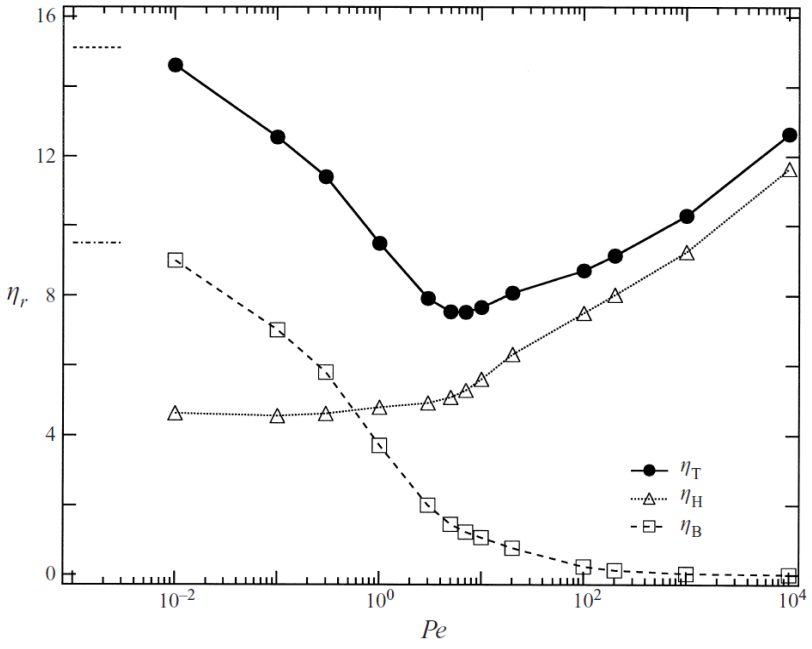

Figure 17 Reduced viscosity as a function of increasing Peclet Number. Horizontal lines on the left describe the viscosity limits for Pe→0. The Brownian contribution η_B causes shear thinning at low Peclet numbers, whereas hydrodynamic effects η_H induce shear thickening for Peclet number Pe >10 [55]

445 The shear rate at which viscosity increases is called critical shear rate by
446 Barnes [7] which is shown in Figure 18.

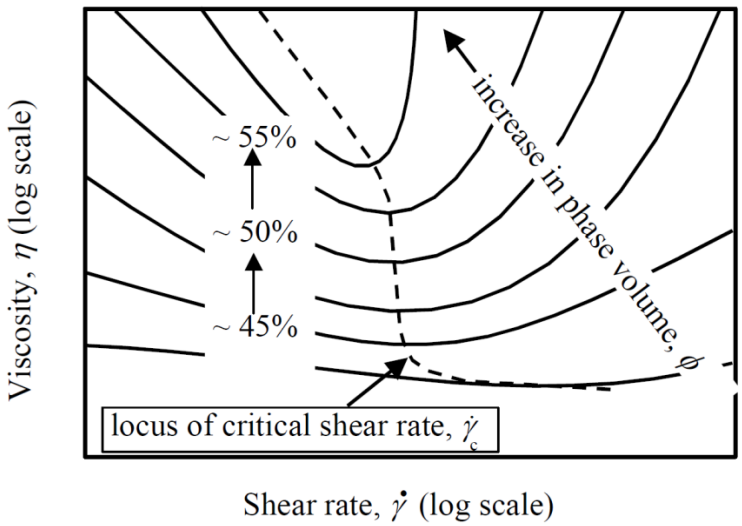

447

448 **Figure 18** The critical shear rate decreases for increasing phase volume [23]

449 The description of shear dependent viscosity by Foss and Brady [55] and Barnes
450 [7] was given for volume fractions of about $\phi = 0.3$ to 0.5, i.e. for considerably
451 higher particle concentrations than it was dealt with in this paper. A locally strong
452 increase of particle fraction due to agglomerates might however explain the
453 findings. Chen et al. [26] describe that aggregation effects can reduce the usual
454 limit for the onset of shear thinning behavior at $\phi \approx 0.2$ below $\phi = 0.1$. Figure 19
455 shows the reduced viscosity of current measurement plotted against the Peclet
456 number, as described by Wager and Brady [54] and Foss and Brady [55]. Note
457 that the onset of shear thickening is observed at about $\mathrm{Pe} \approx 0.1 \ldots 10$, i.e. at about
458 the same order of magnitude for Pe as found in [54,55]. It must be considered
459 that the Peclet number is sensitive to the particle size. Changing the particle
460 diameter for Al_2O_3 to e.g. 130 nm moves the onset of shear thickening to $\mathrm{Pe} \approx 1$.
461 This sensitivity should be considered when discussing the results.

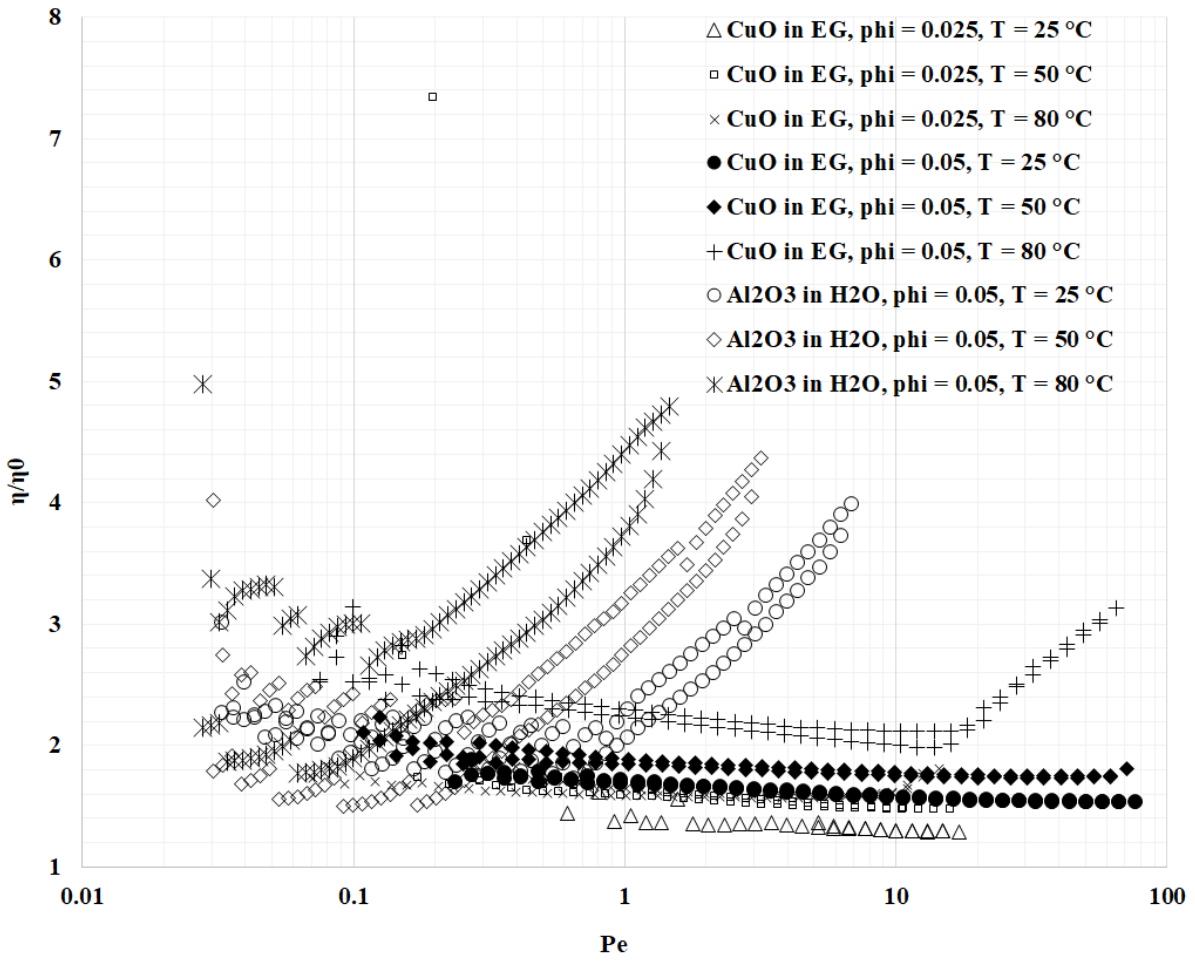

462

463 **Figure 19** Reduced viscosity plotted over Peclet number shows that onset of shear thickening
464 lies in the same order of magnitude as found by Foss and Brady [55].

465 From the explanation and theories that were referred to above from different
466 research groups, it can be concluded that shear thickening is part of the common
467 behavior of suspensions when shear rates increase beyond the critical point.
468 However, this point is dependent on the effective parameters like volume fraction
469 of particles, particles size, particles shape, surfactant etc.

470 # 4. Conclusion

471 The present work has focused on the experimental data on the rheological
472 behavior of different types of nanofluids consisting of Al_2O_3, SiO_2 or CuO
473 particles in water as well as in ethylene glycol under a wide range of shear rate.

By increasing the shear rate in the measurements, all three rheological classes of shear thinning, Newtonian and shear thickening were observed. The explanation of these phenomena can most probably be found in the arrangement of particles. The particles are distributed randomly at very low shear rates, but as the shear rates increase the particles rearrange themselves in a two dimensional layer, which decreases the efficient viscosity of the nanofluids. At higher shear rates, a transition from the mentioned aligned arrangement to a random three dimensional form occurs that leads to the increase in viscosity. So, according to the obtained results and the mentioned discussion, it can be concluded that both shear thinning as well as shear thickening are parts of the common rheological behavior of nanofluids. Yet, this behavior can occur outside of the shear rate range which was investigated, so that nanofluids seem to be of Newtonian or shear thinning nature only. The findings are, however, crucial for research about correlations addressing nanofluids viscosity. Hysteresis effect is also another interesting phenomena which maybe a result of nanoparticles agglomeration, when shear rates are increased and then decreased. Moreover, in order to thoroughly investigate this phenomena, it is strongly recommended to measure viscosity in both directions, from lower shear rate to higher and vice versa.

Data availability

The datasets generated during and/or analysed during the current study are available from the corresponding author on reasonable request.

Acknowledgement

This is a post-peer-review, pre-copyedit version of an article published in International Journal of Thermophysics. The final authenticated version is available online at:
https://doi.org/10.1007/s10765-019-2508-2

References

1. Pinto, R. V., Fiorelli, F. A. S. *Review of the mechanisms responsible for heat transfer enhancement using nanofluids,*Applied Thermal Engineering, 2016, 108, 720-739.
2. Eggers, J.; Kabelac, S. *Radiative Properties of a Nanofluid Mixture, J. Heat Transfer Conference, Kyoto* 2014, **15**, 5712-5725**.**
3. Lapotko, D. *Plasmonic nanoparticle-generated photothermal bubbles and their biomedical applications.* J. Nanomedicine 2009, **4**, 813-845.
4. Mahian, O.; Kianifar, A.; Kalogirou, S. A.; Pop, I.; Wongwises, S. *A review of the applications of nanofluids in solar energy.* J. Heat and Mass Transfer 2013, **57**(2), 582-594.
5. Treopia, C.; Yarin, A. L.; Foss, J. F. *Springer of Experimental Fluid Mechanics,* Springer, 2007.
6. Viswanath, D.S.; Prasad, D. H. L.; Dutt, N.V. K.; Rani, K.Y. *Viscosity of liquids, Theory, Estimation, Experiment, and Data*; Springer: Netherlamd, 2007.
7. Barnes, H.A. *A handbook of elementary rheology*; Institute of Non-Newtonian Fluid Mechanics: University of Wales, 2000.
8. Kirkwood, J.G.; Buff, F.P.; Green, H.S. *The statistical mechanical theory of transport processes. iii. the coefficients of shear and bulk viscosity of liquids.* J. Chemical Physics 1949, **17**(10), 988-994.
9. Kirkwood, J.G. *the statistical mechanical theory of irreversible processes.* J. Nuovo Cimento Supply 1949, **6**(2), 233-236.
10. Born, M.; Green, H.S. *A General Kinetic Theory of Liquids*; Cambridge Uni. Press: London, 1949.
11. Quiñones-Cisneros, S.E.; Deiters, U.K. *Generalization of the Friction Theory for Viscosity Modeling.* J. Physics Chemistry B 2006, **110**, 12820-12834.
12. Quiñones Cisneros, S.E.; Zéberg-Mikkelsen, C.K.; Stenby, E.H. *The Friction Theory (f-theory) for Viscosity Modeling.* J. FLuid Phase Equilibria 2000, **169**, 249-276.
13. Brush, S.G. *Theories of liquid viscosity.* Chemical Reviews 1962, **62**, 513-548.
14. Eyring, H.; Hirschfelder, J.O. *The theory of liquid state.* J. physics Chemistry 1937, **4,** 249-257.
15. Eyring, H. *Viscosity, plasticity and diffusion are examples of absolute reaction rates.* J. Chemical Physics 1936, **4**(4), 283-291.

16. Collins, F.C. *Activation energy of the Eyring theory of liquid viscosity and diffusion.* J. physics Chemistry 1957, **26**(2), 398-400.
17. De Guzman, J. *Relation between fluidity and heat of fusion.* J. Anales Soc. Espan. Fia.Y. Quim 1913, **11**, 353-362.
18. Qun-Fang, L.; Yu-Chen, H.; Rui-Sen, L. *Correlation of viscosities of pure liquids in a wide temperature range.* J. FLuid Phase Equilibria 1997, **140**(1-2), 221-231.
19. Lima, F.W. *The viscosity of binary liquid mixtures.* J. physics Chemistry 1952, **56**, 1052-1052.
20. Tamura, M.; Kurata, M. *Viscosity of binary liquid mixtures.* J. Bulletin of the Chemical Society of Japan 1952, **25**, 32.
21. Hind, R.K.; Mclaughlin, E.; Ubbelohde, U.R. *Structure and viscosity of liquids, Camhore+pyrene mixtures.* J. Transactions of the Faraday Society 1960, **56**, 328-330.
22. Einstein, A. *Eine neue Bestimmung der Moleküldimensionen.* J. Annalen der Physik 1906, **324**(2), 289-306.
23. Einstein, A. *Berichtigung zu meiner Arbeit: „Eine neue Bestimmung der Moleküldimensionen.* J. Annalen der Physik 1911, **339**(3), 591-592.
24. Chen, H.; Ding, Y.; Tan, C. *Rheological behavior of nanofluids.* New Journal of Physics 2007, **9**(367), 1-24.
25. Batchelor, G.K. *The effect of Brownian motion on the bulk stress in a suspension of spherical particles.* J. Fluid Mechanics 1977, **83**, 97.
26. Chen, H.; Ding, A.; Lapkin, A. *Rheological behavior of nanofluids containing tube / rod-like nanoparticles.* J. Powder Technology 2009, **194**, 132-141.
27. Khanafer, K.; Vafai, K. *A critical synthesis of thermophysical characteristics of nanofluids.* J. Heat and Mass Transfer 2011, **57**, 582-594.
28. Mahbubul, L.; Saidur, R.; Amalina, M. *Latest developments on the viscosity of nanofluids.* J. Heat and Mass Transfer 2012, **55**, 874-885.
29. Sundar, L.S.; Sharma, K. V.; Naik, M. T; Singh, M. K. *Empirical and theoretical correlations on viscosity of nanofluids: A review.* J. Renewable and Sustainable Energy Reviews 2013, **25**, 670-686.
30. P.C.Mishra, P. C.; Mukherhjee, S.; Nayak, S. K.; Panda, A. *A brief review on viscosity of nanofluid.* International Nano Letter 2014. **4**(4), 109-120.
31. Prasher, R.; Mukherjee, S.; Nayak, S.K.; Panda, A. M*easurements of nanofluid viscosity and its implications for thermal applications.* J. Applied Physics Letters 2006, **89**(13), 109-120.

32. Chandrasekar, M.; Suresh, S.; Bose, A.C. *Experimental investigations and theoretical determination of thermal conductivity and viscosity of Al_2O_3/water nanofluid.* J. Experimental Thermal and Fluid Science 2010, **34**, 210-216.
33. Anoop, K.B.; Kabelac, S.; Sundararajan, T.; Das, D. K. R*heological and flow characteristics of nanofluids: Influence of electroviscous effects and particle agglomeration.* J. Applied Physics 2009. **106**(3), 43909.
34. Yang, Y.; Oztekin, A.; Neti, S.; Mohapatra, S. P*article agglomeration and properties of nanofluids.* J. of Nanoparticle Research 2012, **14**, 852.
35. Buschmann, M.H. *Thermal conductivity and heat transfer of ceramic nanofluids.* International Journal of Thermal Sciences 2012, **162**, 19-28.
36. Venerus, D.C.; Buongiorno, J.; Christianson, R. *Viscosity measurements on colloidal dispersions (nanofluids) for heat transfer applications.* J. Applied Rheology 2010, **20**(4), 44582.
37. W. Tseng,; Wu, C.H. *Sedimentation, rheology and particle-packing structure of aqueous Al_2O_3 suspensions.* J. Ceramics International 2003. **29**(7), 821-828.
38. Tseng, W.J.; Wu, C.H. *Aggregiation, rheology and electrophoretic packing structure of aqueous Al_2O_3 nanoparticle suspensions. J. Acta Materialia 2000, 50, 3757–3766.*
39. Tseng, W.J.; Tzeng, F. *Effect of ammonium polyacrylate on dispersion and rheology of aqueous ITO nanoparticle colloids. J.* Colloid and Surfaces A 2006, **276**(1-3), 34-39.
40. Davies, J.; Binner, J. G. P. *The role of ammonium polyacrylate in dispersing concentrated alumina suspensions.* J. the Europian Ceramic Society 2000, **20**(10), 1539-1553.
41. Tseng, W.J.; Lin, C.L. *Effects of dispersants on rheological behaviour of $BaTiO_3$ powders in ethanol–isopropanol mixtures.* J. Materials Chemistry and Physics 2003, **80**(1), 232-238.
42. Tseng W. J.; Chen. C-N. *Dispersion and rheology of nickel nanoparticle inks.* J. Materials Science 2006, **41**(4), 1213-1219.
43. Tseng, W.J.; Li, S.Y. *Rheology of colloidal BaTiO3 suspension with ammoniumpolyacrylate as a dispersant.* J. Materials Science and Engineering: A 2002, **333**(1), 314-319.
44. Aladag, B.; Halelfadl, S.; Doner, N.; Mare, T.; Duret, S.; Estelle, P. *Experimental investigations of the viscosity of nanofluids at low temperatures.* J. Applied Energy 2012, **97**, 876-880.

45. Hong, R.Y.; Pan, T. T.; Han, Y. P.; Li, H. Z.; Ding, J.; Han, S. Ma*gneticfield synthesis of Fe_3O_4 nanoparticle used as a precursor of ferrofluids.* J. Magnetism and Magnetic Materials 2007, **310**(1), 37-47.

46. Hong, R.Y.; Etemad, S. Gh. ; Bagheri, R. ; Thibault, J. Rh*eological properties of water-based Fe_3O_4 ferrofluids.* J. Chemical Engineering Science 2007, **62**(21), 5912–5924.

47. Garg, J.; Poudel, B.; Chiesa, M.; Gordon, J. B.; Ma, J. J.; Wang, J. B.; Ren, Z. F.; Kang, Y. T.; Ohtani, H.; Nanda, J.; McKinley, G. H.; Chen. G. E*nhanced thermal conductivity and viscosity of copper nanoparticles in ethylene glycol nanofluid.* J. Applied Physics 2008, **103**, 074301.

48. Hojjat, M.; Etemad, S. Gh.; Bagheri, R.; Thibault, J. *Rheological characteristics of non-Newtonian nanofluids: Experimental investigation.* J. International Communications in Heat and Mass Transfer 2011, **38**, 144-148.

49. Namburu, P.; Kulkarni, D. P.; Misra, D.; Das, D. K. *Viscosity of copper oxide nanoparticles dispersed in ethylene glycol and water mixture.* J. Experimental Thermal and Fluid Science 2007, **32**(2), 397-402.

50. Kole, M.; Dey, T.K. *Thermal conductivity and viscosity of Al_2O_3 nanofluid based on car engine coolant.* J. Physics D 2010, **43**, 315501.

51. Nguyen, C.; Desgranges, F.; Roy, G.; Galanis, N.; Mare, T.; Boucher, S.; Mintsa, H. A. *Temperature and particle-size dependent viscosity data for water-based nanofluids – Hysteresis phenomenon.* J. Heat and Fluid Flow 2007, **28**(6), 1492-1506.

52. Nguyen, C.; Kulkarni, D. P.; Misra, D.; Das, D. K. *Viscosity data for Al_2O_3–water nanofluid—hysteresis: is heat transfer enhancement using nanofluids reliable?* J. Thermal Sciences 2008, **47**, 103-111.

53. Brown, E.; Forman, N. A. ; Orellana, C. S.; Zhang, H.; Maynor, B. W.; Betts, D. E.; DeSimone, J. M.; Jaeger, H. M. *Generality of shear thickening in dense suspensions.* J. Nature Materials 2010, **9**, 220-224.

54. Wagner, N.J.; Brady, J.F.*Generality of shear thickening in dense suspensions.* J. Physics Today 2009, **62**(10), 27-32.

55. Foss, D.R.; Brady, J.F. *Structure, diffusion and rheology of Brownian suspensions by Stokesian Dynamics simulation.* J. Fluid Mechanics, 2000, **407**, 167-200.

56. Phung, T.N.; Brady, J.F.; Bossis, G. *Stokesian Dynamics simulation of Brownian suspensions*. J. Fluid Mech. 1996, **313**,181-207.